LANDSLIDE DETECTION IN CENTRAL AMERICA USING THE DIFFERENTIAL BARE SOIL INDEX

Dr. Alexander Ariza * [a], Dr. Norma Angelica Davila [b], Hannah Kemper [a], Dr. Gerhard Kemper [c]
[a] UN-SPIDER, Bonn/Germany – aariza@ucm.edu.co
[b] UNAM, Mexico City/Mexico – nadavilah@uaemex.mx
[c] GGS GmbH Speyer/Germany – hannah.kemper@ggs-speyer.de

Commission III

KEY WORDS: Landslides, Differential Bare Soil Index, Object-based detection, Disaster Management

ABSTRACT:

The increasing availability of EO data from the Copernicus program through its Sentinel satellites of the medium spatial and spectral resolution has generated new applications for risk management and disaster management. The recent growth in the intensity and number of hurricanes and earthquakes has demanded an increase in the monitoring of landslides. It is necessary to monitor large areas at a detailed level, which has previously been unsatisfactory due to its reliance on the interpretation of aerial photographs and the cost of high-resolution images.
Using the differential Bare Soil Index for optical imagery interpretation in combination with cloud-computing in Google Earth Engine is a novel approach. Applying this method on a recent landslide event in Oaxaca in Mexico around 62% of the landslides were detected automatically, however, there is a big potential for improvement. Including NDVI values and considering images with a higher spatial resolution could contribute to the enhancement of landslide detection, as the majority of missed events have a size smaller than half a pixel. Landslide detection in Google Earth Engine has become a promising approach for big data processing and landslide inventory creation.

1. INTRODUCTION

A landslide is a movements of rocks, earth or debris downhill categorized on the basis of material and type of movement (European Soil Data Centre (ESDAC)). Statistics reveal that landslides caused almost 30.000 fatalities and 40 billion dollars of economic losses in the period of 2000 to 2014 (Valerio Lo Bello, 2017). Several factors have an influence on the occurrence of landslides and are classified whether the trigger is natural like ground vibrations, groundwater pressure or wildfires or human activities being mining, pipe leakages, constructions and soil excavation (Mohan et al., 2020).
Detection of landslides and landslide inventories have been in discussions among scholars for a while. The methods range from geomorphologic field survey and visual analysis of aerial images to remote sensing based approaches like satellite imagery (Mohan et al., 2020). Remote sensing techniques further include Deep Learning and Machine Learning being promising in the subsequent years (Mohan et al., 2020).
The increasing availability of EO data from programs like Copernicus enhance the possibilities to develop new applications of change detection, landslide inventories or the use of AI. Image classification and the automation of workflows is a great way to detect changes in the land cover.
Considering such changes the Differential Bare Soil Index is a well-known indicator used in studies about mapping drought affected areas or urbanizing settlements (Li & Chen, 2014; Ma et al., 2016; Nguyen et al., 2021).

* Contributing author

High soil brightness and low vegetation coverage help to identify uncovered soil areas that could be the result of landslides (Ma et al., 2016).
Converting the DBSI into a workflow, data processing in Google Earth Engine (GEE) is realized for enhancing landslide detection.

2. MATERIALS AND METHOD

2.1 Study area

The study zone is located in one of the world's hotspots affected by intense earthquakes and hurricanes that occurred in 2020 in the districts of San Pedro Totolapa and San Francisco de Ozolotepec in the State of Oaxaca in the state of Mexico (Fig. 1).

2.2 Data Sources

We used the online geospatial and remote sensing cloud computing platform called Google Earth Engine (GEE) (Gorelick et al., 2020), to create Sentinel-2 mosaics. We selected only images between 2020-05-01 and 2020-05-30 for the pre-landslides mosaic, and between 2020-06-20 and 2020-06-28 for post-landslides mosaic in order to avoid clouds and cirrus, and yet attempt to include a large enough search window for full spatial coverage of the area.
In order to validate the methodology applied to Sentinel-1 data, a landslide inventory was constructed base on SPOT-7 images (1.5 m resolution) acquired from May before the earthquake. This product implies a fusion process between a high panchromatic resolution (1.5m) and the multispectral imagery (Table 1).

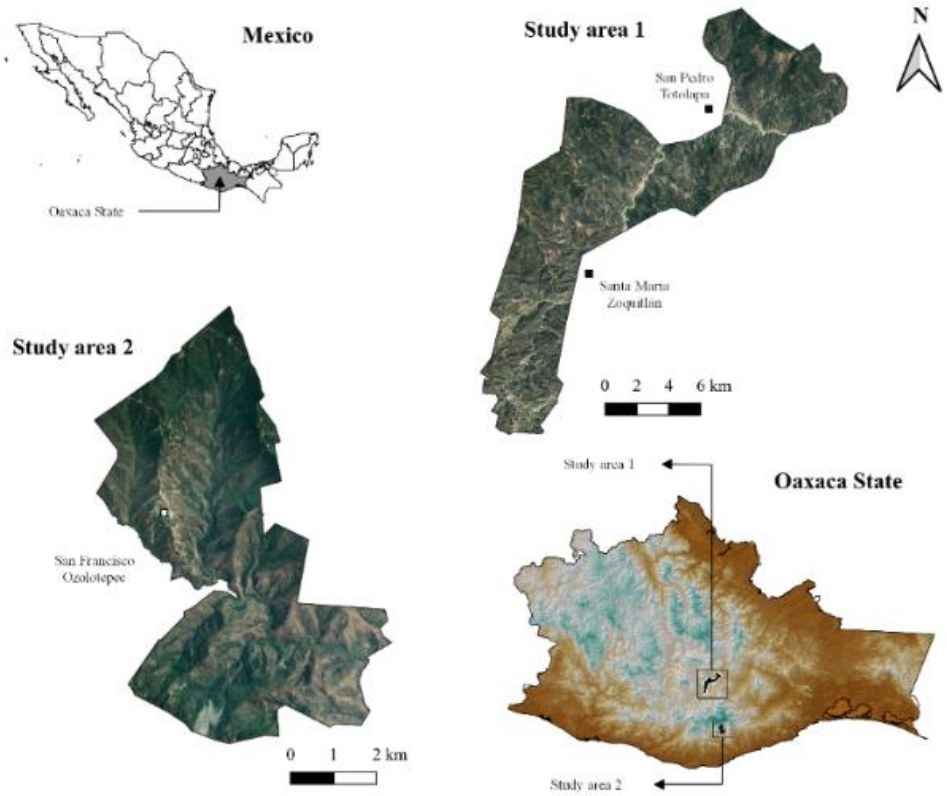

Figure 1. Oaxaca State in Mexico

Table 1. Details of the satellite data used in this study.

Satellite data	Spatial resolution (m)	Date of acquisition
Sentinel-2 A&B	10 m	03/05/2020, 08/05/2020, 13/05/2020, 18/05/2020, 23/05/2020, 28/05/2020, 22/06/2020, and 27/06/2020
SPOT-7	1.5 m	06/27/2020 and 11/09/2020

2.3 Pre-processing of satellite data

The landslide detection using space-based data in these cloud platforms has changed the way to see the risk and to manage the disaster. It aims to facilitate working with big data in the cloud as an alternative to using desktop software. The detailed methodology involved in assessing of landslide detection is presented in Fig. 2

The pre-processing involved filtering the original image collection by specific dates (pre and post), cloud mask (mask2clouds) and, finally, the median values. Next, we will select the bands to build the spectral indices and clip scene images to the study area. To avoid clouds and cirrus clouds, we use cloud masks that are calculated from the three QA bands that are present, we used the QA60 band, which is a bitmask band with cloud mask information, where the bits 10 and 11 are clouds and cirrus, respectively.

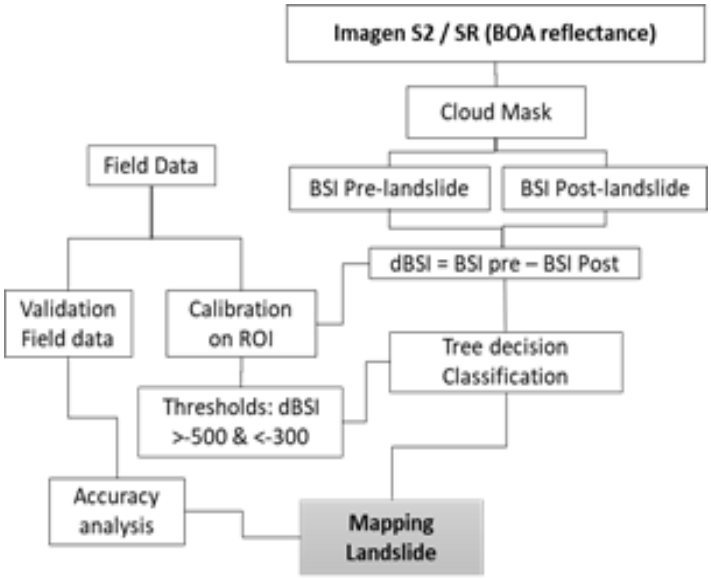

Figure 2. Landslide mapping workflow

2.4 Differential Bare Soil Index (dBSI)

In this study for landslide rapid mapping, we propose to base the response on the Bare Soil Index (BSI) (Roy et al., 1996; Rikimaru & Miyatake, 1997) for the detection of the traces of the soil movements. The BSI is a numerical indicator that combines blue, red, near-infrared and short wave infrared spectral bands to capture soil variations (Figure 3).

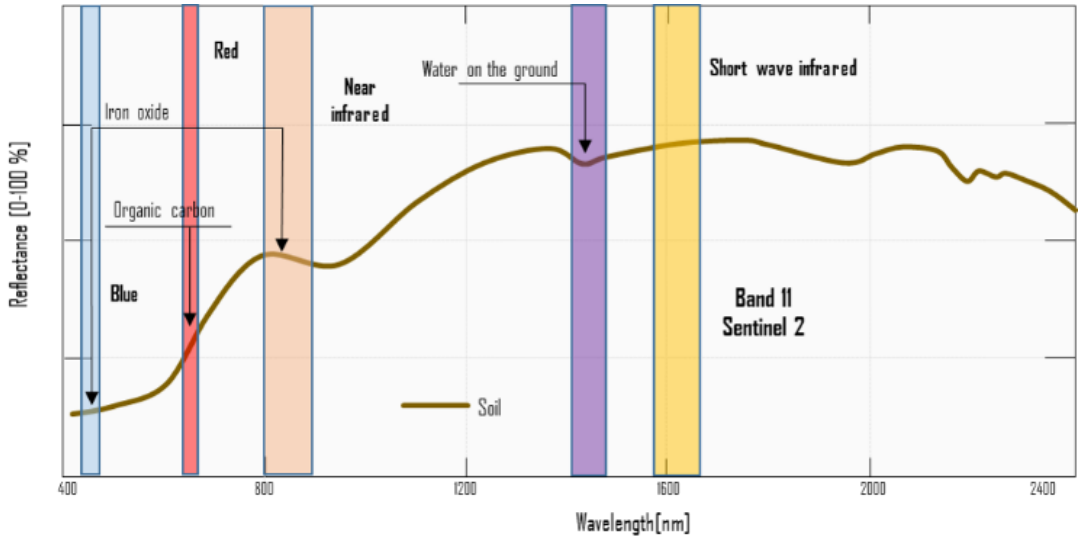

Figure 3. The spectral signature of bare soils associated

These spectral bands are used in a normalized manner. The short wave infrared and the red spectral bands are used to quantify the soil mineral composition, while the blue and the near-infrared spectral bands are used to enhance the presence of vegetation. BSI can be used in numerous remote sensing applications such as soil mapping, crop identification (in combination with NDVI), etc. To calculate the BSI, the following (Equation 1):

$$BSI_{S2}=\frac{(SWIR+Red)-(NIR+Blue)}{(SWIR+Red)+(NIR+Blue)} \quad (1)$$

However, the use of the BSI index itself cannot characterize the landslide configurations on terrain, due to after landslide event, the spectral response changes shortly especially over zones with fast reactivation in the vegetation cover. Therefore, to improve the interpretation of the results.

We use a temporary version or dBSI, this index takes the spectral response before and after the events, to obtain better results of the values of a BSI date linked to the slip targets. Its index is calculated by subtracting the subsequent values of the BSI from the initial values (Equation 2). In the end, the areas with the presence of landslides will appear with negative values. These results are scaled by a factor of 1000 to facilitate their interpretation and range detection.

$$\text{dBSI} = (\text{BSI pre Landslide}) - (\text{BSI Post Landslide}) * 1000 \quad (2)$$

2.5 Detection approach

The first step is the calibration of the differential Bare soil index (dBSI), whose values were taken on areas of interest on the field (AOI) for calibration to extract the value of the interval of the related zones with landslides. Mapping is created by using a tree classifier that identifies areas of bare soil related to landslides (Fig. 2).

In this way, we apply statistical analysis of the value of dBSI on the AOI zones, to extract the value of the interval.

The value of the slip landslide thresholds will be determined by the mean of the dBSI over the AOI + and - one standard deviation (Equation 3):

$$\left| \text{Thr}_{max} = \text{M}_{dBSI} + \text{SD}_{dBSI};\ \text{Thr}_{min} = \text{M}_{dBSI} - \text{SD}_{dBSI} \right| \quad (3)$$

where Thr_{max} and Thr_{min} is the interval of detection, (M_{dBSI}) is the mean of dBSI and (SD_{dBSI}) standard deviation value on AIO zones respectively.

2.6 Accuracy assessment

The accuracy of the classification results derived from the proposed technique by the dBSI, can be expressed using an error matrix (Congalton, 1991), or in terms of branching factor, lack factor, detection percentage and quality percentage (Lee et al., 2003). While the first method is effective when the purpose is to evaluate the accuracy of the classification result of the whole image/area, the second method is effective when the goal is to detect only targets such as landslides from the image. Therefore, in this study, the latter method was selected to estimate the precision figures using the following equations (Lee et al., 2003; Tapas et al., 2012).

$$Branching\ factor\ (BF) = \frac{False\ positive}{True\ positive} \quad (4)$$

$$Miss\ factor\ (MF) = \frac{False\ negative}{True\ positive} \quad (5)$$

$$Detection\ percentage = \frac{True\ positive}{(True\ positive + False\ negative)} * 100 \quad (6)$$

$$Quality\ percentage = \frac{True\ positive}{(True\ positive + False\ negative + False\ positive)} * 100 \quad (7)$$

The branching and missing factors indicate two types of potential errors, that is, false positives and false negatives that can be generated during the automatic detection process. The detection percentage indicates the landslides correctly identified by the proposed methodology. Percent quality, which is the strictest measure of precision among

the four previous precision estimates, indicates the probability that a landslide identified by the methodology is true (Tapas et al., 2012).

True positives, false positives and negatives were calculated by comparing the landslide inventories created semi-automatically by the proposed methodology with the reference inventories, which were created manually using the visual interpretation technique on high resolutions images SPOT-7 (Fig. 4).

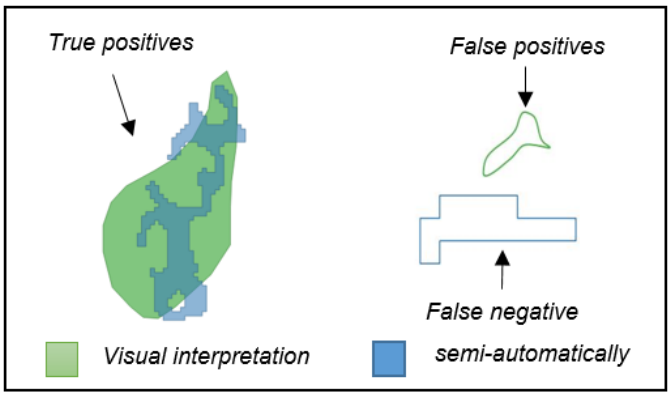

Figure 4. Estimation of the precision: true positives (a), false positives (b) and false negatives (c), for assessing the accuracy of dBSI in landslides.

3. RESULTS AND VALIDATION

From descriptive statistics analysis of the AOI values observed in the field, it was possible to determine the mean (-336.95) and SD (-336.95) values respectively. This indicates that the majority of pixels related to landslides presents BSI values (> 0.7), and in consequence which determines that most of the areas where landslides occur show values between dBSI of -158.17 to 495.12 in the dBSI approximately (Fig. 5).

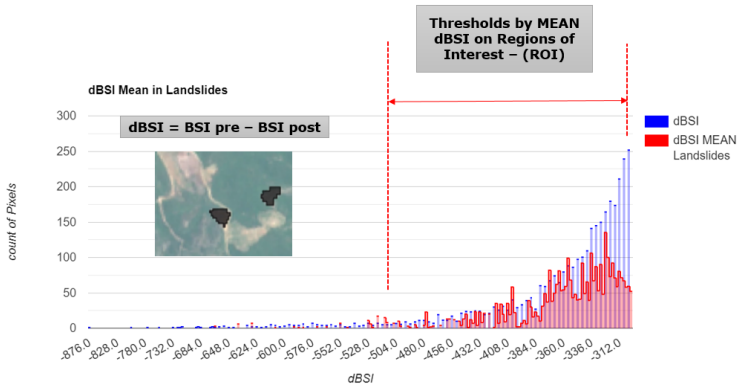

Figure 4. Landslide thresholds of the dBSI

The result of accuracy assessment of the dBSI to landslide detecting, was carried out for the total of landslides detected by the semi-automatic decision tree classification based. Wise accuracy figures for all landslides in the Oaxaca state area and their classification into the different precision types measures are provided in Table 2.

Table 2. Accuracy of dBSI landside detection classifier in the Oaxaca state for the four different precision types

Analysis of area	Visual detection SPOT-7 (ha)	dBSI detection sentinel-2 (ha)	OVERLAP ANALYSIS					
			true positive		false positive		false negative	
			(ha)	%	(ha)	%	(ha)	%
3528,66	12,99	10,94	6,80	52,35	6,19	47,65	4,14	37,86

Differential bared Soil Index - dBSI		
	factor	Value
Branching factor	BF	0,91
Miss factor	MF	0,61
Detection percentage (%)	DP	62,14
Quality percentage (%)	QP	39,69

The results obtained were validated through high-resolution images from SPOT 7. Resulting in an analysis on 3,528.66 ha, where 10.9 ha were detected by the dBSI semi-automatic method, in relation to the 12.9 ha detected by visual interpretation of the AOI on the SPOT-7 image, evidencing that the proposed method is available for detecting approximately 62% of landslides, the main omissions being those less than approximately half a pixel wide. This demonstrates the potential use of dBSI for rapid mapping of landslides in earthquakes or intense hurricanes, using Sentinel-2 images provided which are free of shadows, cirrus and clouds in the study areas.

The performance of the methodology to detect landslides is moderately good. Particularly for Sentinel 2 images, both for its detection capacity, if not also for t the Miss factor (MF) for this is also lower compared to other methodologies (Tapas et al., 2011). This is mainly due to the identification of changes in vegetation as false positives.

CONCLUSION

The differential Bare Soil Index proposed (dBSI) in this study, was developed to detect the traces of the ground movements after earthquake. As complementary method to support traditional interferometric-SAR analysis.

The preliminary results showed that the use of dBSI is sufficient to identify recent traces of soil movements useful for rapid mapping response during a disaster event. In this case, the use of the dBSI index itself has not been able to characterize the landslide configurations on terrain, due to after landslide event, the spectral response changes shortly especially over zones with fast reactivation in the vegetation cover. Therefore, to improve the interpretation of the results, we recommended the use of another index like NDVI or SAVI in the analysis (pre and post events) to eliminate the vegetation change effects and get better outcomes of BSI values linked to landslide targets. Unfortunately, it also highlights certain clouds, cirrus clouds, making it difficult to separate areas of bare ground from other covers. These results are highly dependent on vegetation change, seasonal agriculture, and cloud-free images.

ACKNOWLEDGMENTS

The completion of field observation on this paper could not have been possible without the participation and assistance of other members of this project.

A special thanks is dedicated to UN SPIDER in Bonn.

REFERENCES

Congalton, R.G., 1991. A review of assessing the accuracy of classifications of remotely sensed data. Remote Sensing of Environment 37 (1), 35–46.

European Soil Data Centre (ESDAC): Landslides. https://esdac.jrc.ec.europa.eu/

Gorelick, N., Hancher, M., Dixon, M., Ilyushchenko, S., Thau, D., Moore, R., 2017. Google earth engine: planetary-scale geospatial analysis for everyone. Remote Sens. Environ. 202, 18-27. https://doi.org/10.1016/j.rse.2017.06.031.

Lee, D.S., Shan, J., Bethel, J.S., 2003. Class-guided building extraction from Ikonos imagery. Photogrammetric Engineering and Remote Sensing 69 (2), 143–150.

Li, S.; Chen, X., 2014. A new bare-soil index for rapid mapping developing areas using LANDSAT 8 data. Int. Arch. Photogramm. Remote Sens. Spatial Inf. Sci. XL-4,139–144.

Ma, H.; Xinwen, C.; Chen, L.; Zhang, H.; Xiong, H., 2016. Automatic identification of shallow landslides based on Wordview2 remote sensing images. Journal of Applied Remote Sensing 10.1.

Mohan, Amrita; Singh, Amit Kumar; Kumar, Basant; Dwivedi, Ramji. 2020. Review on remote sensing methods for landslide detection using machine and deep learning. Trans Emerging Tel Tech. DOI: 10.1002/ett.3998.

Nguyen, Can Trong; Chidthaisong, Amnat; Kieu Diem, Phan; Huo, Lian-Zhi, 2021. A Modified Bare Soil Index to Identify Bare Land Features during Agricultural Fallow-Period in Southeast Asia Using Landsat 8. Land 10 (3).

Valerio Lo Bello (2017): Landslide Hazard and Risk Assessment. Ed. UNISDR.

Rikimaru, A., & Miyatake, S., 1997. Development of forest canopy density mapping and monitoring model using indices of vegetation, bare soil and shadow, presented paper for the 18th ACRS. Kuala Lumpur, Malaysia.

Rodríguez-Pérez, Q., Márquez-Ramírez, V. H., and Zúñiga, F. R. 2020: Seismicity characterization of oceanic earthquakes in the Mexican territory, Solid Earth, 11, 791–806, https://doi.org/10.5194/se-11-791-2020, 2020.

Roy, P. S., Sharma, K. P., & Jain, A., 1996. Stratification of density in dry deciduous forest using satellite remote sensing digital data—An approach based on spectral indices. Journal of biosciences, 21(5), 723-734.

Tapas R. Martha, Norman Kerle, Cees J. van Westen, Victor Jetten, K. Vinod Kumar, 2012. Object-oriented analysis of multi-temporal panchromatic images for creation of historical landslide inventories. ISPRS Journal of Photogrammetry and Remote Sensing, Volume 67.105-119.

van Westen, C.J., Castellanos, E., Kuriakose, S.L., 2008. Spatial data for landslide susceptibility, hazard, and vulnerability assessment: an overview. Engineering Geology 102 (3–4), 112–131.